

**Technical note: The use of an interrupted-flow  
centrifugation method to characterise preferential flow in  
low permeability media**

**Richard A. Crane,<sup>1,2\*</sup> Mark O. Cuthbert<sup>2,3</sup> and Wendy Timms<sup>2,4</sup>**

[1] School of Civil and Environmental Engineering, UNSW, Australia

[2] Connected Waters Initiative Research Centre, UNSW, Australia

[3] School of Geography, Earth and Environmental Sciences, University of Birmingham,  
United Kingdom

[4] School of Mining Engineering, UNSW, Australia

Correspondence to: R. A. Crane (r.crane@unsw.edu.au)

23   **Abstract**

24   We present an interrupted-flow centrifugation technique to characterise preferential flow in  
25   low permeability media. The method entails a minimum of three phases: centrifuge induced  
26   flow, no flow and centrifuge induced flow, which may be repeated several times in order to  
27   most effectively characterise multi-rate mass transfer behaviour. In addition, the method  
28   enables accurate simulation of relevant in situ total stress conditions during flow by selecting  
29   an appropriate centrifugal force [level](#). We demonstrate the utility of the technique for  
30   characterising the hydraulic properties of smectite clay dominated core samples. All [core](#)  
31   samples exhibited a non-Fickian tracer breakthrough (early tracer arrival), combined with a  
32   decrease in tracer concentration immediately after each period of interrupted-flow. This is  
33   indicative of dual (or multi) porosity behaviour, with solute migration predominately via  
34   advection during induced flow, and via molecular diffusion (between the preferential flow  
35   network(s) and the low hydraulic conductivity domain) during interrupted-flow. Tracer  
36   breakthrough curves were simulated using a bespoke dual porosity model with excellent  
37   agreement between the data and model output (Nash–Sutcliffe model efficiency coefficient  
38   was >0.97 for all samples). In combination interrupted-flow centrifuge experiments and dual  
39   porosity transport modelling are shown to be a powerful method to characterise preferential  
40   flow in low permeability media.

41

42

43

44

45

46

47   **Key words:** dual porosity, interrupted flow, centrifugation, solute transport, molecular  
48   diffusion

49

50

## 51 Introduction

52 It is well known that heterogeneities, including biogenic pores/channels, desiccation cracks,  
53 fissures, fractures, non-uniform particle size distributions and inter-aggregate pores, are  
54 widespread in the subsurface and lead to a range of preferential flow phenomena (Beven and  
55 Germann, 1982; Cuthbert et al., 2013; Cuthbert and Tindimugaya, 2010; Flury et al., 1994).  
56 The coexistence of relatively high hydraulic conductivity ( $K$ ) domain(s) and an impermeable  
57 one, often termed dual porosity, results in a non-Fickian breakthrough curve. Solute transport  
58 in such systems is often characterised by an early arrival of solutes originating from the more  
59 mobile domain (macropores) and a slow approach to the final concentration caused by  
60 diffusion into the immobile domain (matrix or microporous network). When fitting  
61 breakthrough curves, therefore, it is often difficult to differentiate between contributions from  
62 the micro- and macropore transport mechanisms. As a consequence, in recent years there has  
63 been much research into the development of effective empirical and modelling techniques to  
64 characterise solute transport processes for dual porosity systems. One method investigated  
65 has been the use of interrupted-flow solute break-through experiments. Amongst the original  
66 work on this topic Murali and Aylmore, (1980) discussed the influence of non-constant flow  
67 on solute transport in aggregated soil. Brusseau et al., (1989) developed a flow-interruption  
68 method for use in measuring rate-controlled sorption processes in soil systems, which was  
69 subsequently applied by Koch and Fluhler, (1993) to investigate advection and diffusion  
70 phenomena occurring for nonreactive solute transport in aggregated media. The idea  
71 proposed was that by interrupting flow during nonreactive tracer breakthrough the degree of  
72 non-equilibrium between any fast and slow flow pathways can be determined. Central to this  
73 hypothesis is that the magnitude of the change in nonreactive tracer concentration in effluent  
74 samples taken immediately after a no-flow period is indicative of such non-equilibrium.  
75 Subsequent work within this field has included: determination of physical (e.g., diffusive  
76 mass transfer between advective and nonadvective water) and chemical (e.g., nonlinear  
77 sorption) nonequilibrium processes in soil (Brusseau et al., 1997); determination of  
78 nonreactive solute exchange between the matrix porosity and preferential flow paths in  
79 fractured shale (Reedy et al., 1996); quantifying the effect of aggregate radius on diffusive  
80 timescales in dual porosity media (Cote et al., 1999); numerical modelling of aqueous  
81 contaminant release in non-equilibrium flow conditions; (Wehrer and Totsche, 2003)  
82 empirical modelling of the release of dissolved organic species (Guimont et al., 2005; Ma and  
83 Selim, 1996; Totsche et al., 2006; Wehrer and Totsche, 2005; Wehrer and Totsche, 2009) and

Formatted: Font: Italic

heavy metals (Buczko et al., 2004); increasing the efficiency of solute leaching (Cote et al., 2000); empirical modelling of conservative tracer transport in a laminated sandstone core sample (Bashar and Tellam, 2006); and characterising in situ aquifer heterogeneity (Gong et al., 2010). One area where comparatively few studies exist, however, is in characterising the hydraulic properties of aquitards (e.g. clay dominated soils and sediments, shales, mudstones). ~~Such research is of particular interest, which because may have~~ preferential flow paths, ~~which by their intrinsic nature, can significantly~~ compromise the integrity of aquitard units as local and regional barriers to the movement of groundwater contaminants. There are, ~~presently,~~ significant technical difficulties at present, however, in characterising such features at appropriate scales (Cuthbert et al., 2010). For example, it is well known that the ~~hydraulic conductivity~~ *K* of glacial till is scale dependent, with laboratory permeability measurements often yielding values ~~orders of magnitude~~ lower than field based measurements and modelling (Cuthbert et al 2010). As a consequence a key requirement of laboratory scale aquitard characterisation is that the core sample must be of sufficient volume in order to incorporate the key dual porosity features which govern the overall formation. A second technical challenge is that laboratory testing typically requires generation of flow through the sample whilst maintaining relevant in situ hydro-geotechnical conditions. One method which has been demonstrated as effective for this purpose is centrifugation, which is increasingly being used for hydraulic and geotechnical testing of low *K* materials (Hensley and Schofield., 1991; Nimmo and Mello., 1991; Timms et al., 2009; Timms and Hendry., 2008). Moreover, experiments using geotechnical centrifuges with payload capacities exceeding several kilograms can provide the additional benefit of being able to use core samples of representative scale for the overall formation. Here we present, for the first time, an interrupted-flow methodology using a centrifuge permeameter (CP) to characterise possible dual porosity behaviour of low permeability porous media. A novel dual domain model is also described which has been used to guide physical interpretation of the experimental tracer breakthrough curves.

Formatted: Font: Italic

## 2. Experimental methods

### 2.1. Core and groundwater sampling methodology

The clay core (101.6 mm in diameter, Treifus core barrel, non-standard C size) and groundwater were sourced from a 40 m thick, semi-consolidated, clay-rich alluvium deposit located approximately 100 km south of Gunnedah, New South Wales, Australia (31° 31'9"S, 150° 28'7"E). Equipment and procedures for obtaining minimally disturbed cores were

compliant with ASTM (2012). See Timms et al., (2014) for a review of the procedure. Groundwater samples were taken from piezometers using standard groundwater quality sampling techniques (Sundaram et al., 2009). A 240V electric submersible pump (GRUNDFOS MP1) and a surface flow cell were used to obtain representative samples after purging stagnant water to achieve constant field measurements of electrical conductivityEC, pH, dissolved oxygen (DO) and reduction potential (Eh).

## 2.2. Centrifuge permeameter theory

During centrifugation increased centrifugal force generates a body force which accelerates both solid and fluid phases within the sample. Centrifugal acceleration at any point within a centrifuge sample is calculated as follows:

$$a = \omega^2 r \quad \text{Eq. (1)}$$

Where  $a$  is the centrifugal acceleration ( $\text{m/s}^2$ ),  $\omega$  is the angular velocity (radian/s), and  $r$  is the radius from the axis of rotation (m). The  $g$ -level is the scaling factor ( $a/g$ ) for accelerated gravity, where  $g$  is gravity at the Earth's surface.

Vertical hydraulic conductivity,  $K_v$  (m/s) is calculated using ASTM (2000) (Eq. 2), where:  $Q$  = the steady-state fluid flux (mL/h);  $A$  = the sample flow area ( $\text{cm}^2$ );  $r_m$  = the radial distance at the mid-point of the core sample (cm); and RPM = revolutions per minute.

$$K_v K = \frac{0.248Q}{Ar_m(RPM)^2} \quad \text{Eq. (2)}$$

The estimated in situ stress applied at the base of the core samples was calculated according to Eq. 3, and assumes that the overlaying formations were fully saturated and of a similar density to the core samples.

$$\sigma_i = \rho_s dg \quad \text{Eq. (3)}$$

Where  $\sigma_i$  = in situ stress (kPa);  $\rho_s$  = saturated density of core ( $\text{kg/m}^3$ );  $d$  = depth to the base of the core sample (m BGL); and  $g$  = gravitational acceleration ( $\text{m/s}^2$ ). The applied stress at

Formatted: Font: Not Italic

Formatted: Subscript

the base of the core ( $\sigma_g$ , kPa) during the centrifuge experiments was calculated according to Eq. 4 (Timms et al. 2014).

$$\sigma_g = [(\rho_b L_c) + \rho_w(L_c + h_w)]a_b \quad \text{Eq. (4)}$$

where  $\rho_b$  = core bulk density ( $\text{kg/m}^3$ );  $L_c$  = length of CP core specimen (mm);  $\rho_w$  = influent density ( $\text{kg/m}^3$ );  $h_w$  = height of influent water above CP core specimen (mm); and  $a_b$  is the centrifugal acceleration at the base of the CP core specimen.

### 2.3. Centrifuge permeameter sample preparation

A Broadbent geotechnical centrifuge (GMT GT 18/0.7 F) with a custom built permeameter module (Timms et al., 2014) was used for this study. Prior to mounting into the CP the outer 5 mm of the clay cores were trimmed and the trimmed cores were then inserted into Teflon cylindrical core holders (100 mm internal diameter, 220 mm length) using a custom built mechanical cutting and loading device. The cores were trimmed in order to remove any physical and chemical disturbance associated with the core extraction (drilling) process. A 5 mm thick A14 Geofabrics Bidim geofabric filter (100 micron,  $K = 33 \text{ m/s}$ ) was placed above and below the sample in order to prevent clogging of the effluent drainage plate with colloid material from the sample. The geofabric filter was held in position above the sample using a plastic clamp.

Formatted: English (U.S.)

The core holders (with the core sample held within) were placed into 3000 mL glass beakers containing 1000 mL of groundwater derived from the piezometer at the closest depth to the core sample (see Table 1) and allowed to saturate from the base upwards. In total three core samples were analysed, which were taken from depths of 5.03, 9.52 and 21.75 m BGL. This Saturation was performed by immersing the core holder into a reservoir of groundwater with the level of the water 5 cm higher than the top of the core sample. The mass of each core was then monitored every 24 hours until no further increase in mass was recorded, saturation was then assumed to have occurred. The core holders (containing the saturated core samples) were mounted to the CP system via double O-ring seals. An influent head was added to all samples (see Table 1), which was maintained during centrifugation by a custom built automated influent level monitoring and pumping system. The system comprises ~~of~~ a carbon fibre EC electrode array which is connected via a fibre optic rotary joint to a peristaltic pump

that supplies influent from an external 100 mL burette. Effluent samples were collected in an effluent reservoir and extracted using a 50 mL syringe. All experiments were conducted under steady-state flow, which is defined as a <10% difference between influent and effluent flow rates. The influent volume was determined by manual measurements of the water level in the external burette and effluent volumes were measured by multiplying their mass by their density.

Formatted: English (U.S.)

## 2.4. Interrupted-flow experiment methodology

The idea of interrupting the flow during a breakthrough experiment is to differentiate between advection and diffusion processes. The method comprises a minimum of three phases:

1. Flow is induced at a constant centrifugal force for a fixed time period with effluent samples collected at multiple periodic intervals. The  $g$ -level and influent reservoir height are selected so that the maximum total stress on the core approached the estimated in situ stress of the material at the given depth in the formation (Eq. 3 and 4). The time period between each effluent sampling interval is selected in order to gain sufficient effluent volume (namely >1 mL) for accurate volume and nonreactive tracer concentration measurement.
2. Flow is interrupted (stopped) for a fixed time period during which time the permeameters are disconnected from the centrifuge module and positioned upright, the influent reservoir is also removed to limit any downward migration of solutes. A relatively long interrupted-flow period (>12 hrs) is selected so that slow mass transfer processes can be identified.
3. Phase 1 is then repeated.

All phases can be repeated multiple times in order to record sufficient non-reactive tracer breakthrough which enables the mass transport behaviour to be accurately characterised. Deuterium oxide ( $D_2O$ ) (Acros Organics, 99.8% concentration) was used as a non-reactive tracer. A concentration of 3.12 mL/L was used, which raised the concentration of  $D_2O$  to approximately 200%. This was selected as sufficiently high in order to result in accurately measureable mass transfer changes. Effluent samples were filtered using a 0.2  $\mu m$  cellulose acetate filter, stored at 4 °C and analysed for  $\delta D$  within 7 days of testing.  $\delta D$  was determined by measuring the  $^1H/^2H$  ratio to an accuracy of 0.1% using a Los Gatos DLT100 isotope analyser.

## 2.5. Dual domain transport modelling

Dual porosity models were created using COMSOL Multiphysics (v. 4.4) modified from well-known formulations described, for example, by Coats and Smith, (1964), and Bear (1987) and Gerke and van Genuchten, (1993). The purpose of the modelling was to aid physical interpretation of the tracer breakthrough curves and validate the hypothesis that the step changes in tracer concentrations observed during no-flow periods could be explained by the presence of dual porosity in the samples. The models comprised a classical advection-dispersion equation for a mobile zone (subscript  $m$ ) representing preferential flow pathways with a source/sink term representing exchange of solute with an immobile zone (subscript  $im$ ). Solute transport in the immobile zone was by diffusion only. The exchange flux between the immobile and mobile zones was modelled as being proportional to the concentration difference between the zones. The governing equations are as follows:

$$\frac{\partial C_m}{\partial t} = D_m \frac{\partial^2 C_m}{\partial z^2} - \frac{q(t)}{\phi_m} \frac{\partial C_m}{\partial z} - \frac{\gamma}{\phi_m} (C_m - C_{im}) \quad (\text{Eq. 5})$$

$$\frac{\partial C_{im}}{\partial t} = \mu \frac{\partial^2 C_{im}}{\partial z^2} + \frac{\gamma}{\phi_{im}} (C_m - C_{im}) \quad (\text{Eq. 6})$$

$$D_m = \frac{\alpha q(t)}{\phi_m} + \mu \quad (\text{Eq. 7})$$

where  $C$  is the  $\delta D$  isotope ratio [1],  $t$  is time [T],  $z$  is distance along the column [L],  $q$  is fluid flux [ $LT^{-1}$ ],  $\alpha$  is hydrodynamic dispersivity [L],  $\mu$  is the coefficient of molecular diffusion [ $L^2T^{-1}$ ]. The porosity,  $\phi$ , of the mobile and immobile domain is defined as:

$$\phi_m = \frac{V_{p,m}}{V_T} \quad (\text{Eq. 8})$$

$$\phi_{im} = \frac{V_{p,im}}{V_T} \quad (\text{Eq. 9})$$

where  $V_{p,m}$  is the pore volume of the mobile domain [L],  $V_{p,im}$  is the pore volume of the immobile domain [L] and  $V_T$  is the total volume of the saturated core [L]. The mass transfer coefficient,  $\gamma$  [ $T^{-1}$ ], is defined as:

$$\gamma = \frac{\beta \phi_m \mu}{a^2} \quad (\text{Eq. 10})$$

231 where  $\beta$  is the dimensionless geometry coefficient, which typically ranges from 3 for  
232 rectangular slabs to 15 for spherical aggregates, and  $a$  is the characteristic half width of the  
233 matrix block [L] (Gerke and van Genuchten, 1993).

234 The initial concentration conditions were set to zero for both domains for all model runs.  
235 During centrifugation periods, a variable solute flux upper boundary condition was used for  
236 the mobile domain varied according to the product of the measured fluid flux & input  
237 concentration ( $C_0$ ) during each experiment as follows:

238 
$$\frac{q(t)}{\phi_m} C_0 = \frac{q(t)}{\phi_m} C_m + D_m \frac{\partial C_m}{\partial z} \quad (\text{Eq. 11})$$

239 A Dirichlet (constant concentration) upper boundary condition was used for the immobile  
240 domain during times of centrifugation. A novel aspect of the models, facilitated by the  
241 flexibility of model structure variations possible in COMSOL, was that the upstream  
242 transport boundary for both domains was switched to a zero flux condition during the  
243 interrupted flow phases. The downstream transport boundary conditions for both domains  
244 were given by:

245 
$$\frac{\partial C_{m,im}}{\partial z} = 0 \quad (\text{Eq. 12})$$

246 At  $z = L$ , where  $L$  was sufficiently large to ensure the results at the column outlet distance (at  
247  $z \ll L$ ) were not sensitive to the position of the boundary. Variable flux boundary conditions  
248 were used for both flow and transport into the mobile domain and  $q$  varied according to the  
249 measured flow rate during each effluent sampling interval. A novel aspect to the models,  
250 facilitated by the flexibility of model structure variations possible in COMSOL, was that the  
251 upstream transport boundary for the immobile zone was defined using a Dirichlet (constant  
252 concentration) condition during times of centrifugation, but switched to a no-flow condition  
253 during the interrupted flow phases. The downstream transport boundary flux was set equal to  
254 the sum of the advective and diffusive flux components at a large distance downstream to  
255 ensure the results at the column outlet distance were not sensitive to its position. The total  
256 mass flux at the distance from the upstream boundary corresponding with the length of the  
257 experimental column was output from the models and integrated over the sampling periods  
258 for comparisons to the observed breakthrough curves.  $\mu$  was calculated as  $3.43 \times 10^{-5} \text{ m}^2/\text{d}$   
259 which is the diffusion coefficient of  $\text{D}_2\text{O}$  in  $\text{H}_2\text{O}$  at  $25.0^\circ\text{C}$  (Orr and Butler, 1935) multiplied  
260 by the average tortuosity of 0.15 reported by (Barnes and Allison, 1988) for clay bearing

**Formatted:** Font: (Default) Times New Roman, 12 pt

**Formatted:** Space After: 10 pt, Line spacing: 1.5 lines

**Formatted:** Font: (Default) Times New Roman

**Formatted:** Font: (Default) Times New Roman, 12 pt

**Formatted:** Font: (Default) Times New Roman, 12 pt

**Formatted:** Space After: 0 pt, Don't adjust space between Latin and Asian text, Don't adjust space between Asian text and numbers

media. Model output was fitted to the observed data by varying the unconstrained parameters:  $\alpha$  and  $\gamma$ . Note that  $\emptyset_m$  and  $\emptyset_{im}$  were also considered unconstrained parameters, but their sum was constrained to equal the  $\emptyset_T$  measured for each sample by oven drying at 105°C for 24 hours. In order to quantify the deviation between the recorded data and the dual porosity model the normalised root-mean-square error (NRMSE) and the Nash–Sutcliffe model efficiency coefficient (NSMEC) were calculated (Nash and Sutcliffe, 1970). The mesh size and model tolerance were set sufficiently small so that the results were no longer sensitive to further reduction to ensure the accuracy of the model output. The models runs presented were all executed using an extra fine mesh size and a relative tolerance of 0.00001.

## 2.6. Dual domain model sensitivity testing

Sensitivity analysis of the dual domain model (for the core taken from 5.03 m) was conducted in order to determine how sensitive the model was to changes in the constrained ( $L$ ,  $\emptyset$  and  $\mu$ ) and unconstrained ( $\emptyset_m$ ,  $\alpha$  and  $\gamma$ ) parameters. Sensitivity factors for constrained parameters were determined according to the estimated percentage error associated with each parameter, whilst  $\pm 50\%$  was selected for the unconstrained parameters in order to determine their influence on the NSMEC. The percentage error for  $L$  was calculated to be  $\pm 2.78\%$  due to the core length being 36 mm and the error associated with measurement at each end was  $\pm 0.5$  mm. The percentage error for  $\emptyset$  was calculated to be  $\pm 2.79\%$  which comprises the  $L$  measurement error plus 0.0026% which is the calculated error associated with the two mass measurements. The percentage error for  $\mu$  was determined to be  $\pm 50\%$  due to the range in tortuosity of 0.1 – 0.2 documented by Barnes and Allison, (1988) and references therein.

## 3. Results and discussion

### 3.1. D<sub>2</sub>O breakthrough

D<sub>2</sub>O breakthrough data and best fit dual porosity model output for the interrupted-flow experiments conducted using core samples taken from 5.03 m, 9.52 m and 21.75 m depth BGL are displayed in Fig. 1. A close fit was achieved between the dual porosity model output and the original data, with a NSMEC of 0.97, 0.99 and 0.97 recorded for D<sub>2</sub>O breakthrough data from core samples taken from 5.03 m, 9.52 m and 21.75 m depth BGL respectively. The D<sub>2</sub>O breakthrough curves for all core samples exhibited a relatively elongated shape, with 100% breakthrough not recorded for any of the timescales tested. This was expected given that a ‘long tailing’ is a common feature of dual (or multi) porosity materials, i.e. systems where the mobile domain is coupled to a less mobile, or immobile, domain. In such instances

the dominant solute transport mechanism during imposed flow in the mobile domain(s) is typically advection, however, solute exchange also occurs in parallel with the immobile domain(s), typically via molecular diffusion. Following each interrupted-flow (no flow) period a decrease in  $\delta D$  was recorded for all samples, and attributed to the diffusion of  $D_2O$  from the preferential flow domain(s) into the low-flow (or immobile) flow domain(s). The shape of the  $D_2O$  breakthrough curves and the magnitude of the  $\delta D$  decrease following the interrupted-flow periods are different for all samples, with a 42.6%, 18.5% and 28.4% decrease recorded for the core samples taken from 5.03 m, 9.52 m and 21.75 m depth BGL respectively after the first interrupted-flow period. In addition, the  $K_v$  of each sample was recorded as different (Fig. 2), with average values of  $1.4 \times 10^{-8}$  m/s,  $3.9 \times 10^{-9}$  m/s and  $2.7 \times 10^{-9}$  m/s for the core samples taken from 5.03 m, 9.52 m and 21.75 m depth BGL respectively. The  $K_v$  was recorded to decrease during the initial stages of each centrifugation period, and attributed to the partial consolidation of the clay due to the stress applied by the centrifugal force. Following this initial consolidation period a more constant  $K_v$  as a function of time was recorded for all cores, indicating that relative equilibrium had been achieved between stress applied by the centrifugal force and the compaction state of the core.

Core depth (m BGL)	Estimated in situ total stress, $\sigma_t$ (kPa)	Influent groundwater depth (m BGL)	Influent EC ( $\mu S/cm$ )	$g$ -level applied	Core length, $L_c$ (mm)	Height of influent water above core, $h_c$ (mm)	$K_v$ ( $ms^{-1}$ )	Total stress at base of core during centrifugation, $\sigma_g$ (kPa)
5.03	89	10	18470	20	36	61	$1.4 \times 10^{-8}$	75
9.52	177	10	18470	20	47	81	$3.9 \times 10^{-9}$	127
21.75	383	20	13160	80	54	48	$5.1 \times 10^{-9}$	373

Table 1. Core and influent properties, experimental parameters and  $K_v$  results for the interrupted-flow experiments. Calculations are based on Eq. 2 for  $K_v$ , Eq. 3 for estimated in situ total stress and Eq. 4 for total stress at the base of core specimen during centrifugation.

### 3.4.2. Dual domain model

The close model fits confirm that preferential flow through a dual porosity structure is a plausible hypothesis to explain the shape of the observed breakthrough curves. The unconstrained ( $\phi_m$ ,  $\alpha$  and  $\gamma$ ) parameters that yielded the best dual domain model output fit to the D<sub>2</sub>O breakthrough data are displayed in Table 2. It is noted that the pore volume of the mobile domain per total volume of the core,  $\phi_m$ , was modelled to be 0.04, 0.04 and 0.08 for core taken from 5.03 m, 9.52 m and 21.75 m depth BGL respectively. With total porosity,  $\phi$ , measured as 0.44, 0.47 and 0.43, this equates to 9.1%, 8.5% and 18.6% of the total pore volume respectively, suggesting that preferential flow features comprise a relatively large proportion of the total pore porosity in each sample. Hydrodynamic dispersivity,  $\alpha$ , for best fit model output for all core samples was  $L/2$ , which is larger than typically reported for laboratory scale column experiments (e.g. Shukla et al., 2003). It can be noted that all of the core samples were assumed to have remained saturated throughout the breakthrough experiments because all influent and effluent flow rates were recorded at steady-state. Whilst dispersion is known to increase substantially as moisture content decreases from saturation (e.g. Wilson and Gelhar, 1981) it is therefore unlikely that this could have been a factor. The mass transfer coefficient,  $\gamma$ , was also modelled as different for each core sample with 0.65, 1.50 and 1.20 yielding the best model fit for the core samples taken from 5.03 m, 9.52 m and 21.75 m depth BGL respectively. Using Eq. 10 the half width of the matrix block (using a  $\beta$  range of 3-15 (for 3 for parallel slabs and 15 for spherical aggregates an idealised parallel fracture geometry after Gerke and van Genuchten, (1993)),  $a$ , is calculated as within the range of 8.0-17.8 mm, 5.4-12.1 mm and 5.5-12.3 mm for the core samples taken from 5.03 m, 9.52 m and 21.75 m depth BGL respectively. This suggests that the preferential flow channels present are likely to be separated by distances in the order of several mm from each other within the cores. With the dimensions of the cores significantly greater than these values the model output therefore suggests that several preferential flow features are present in each core sample.

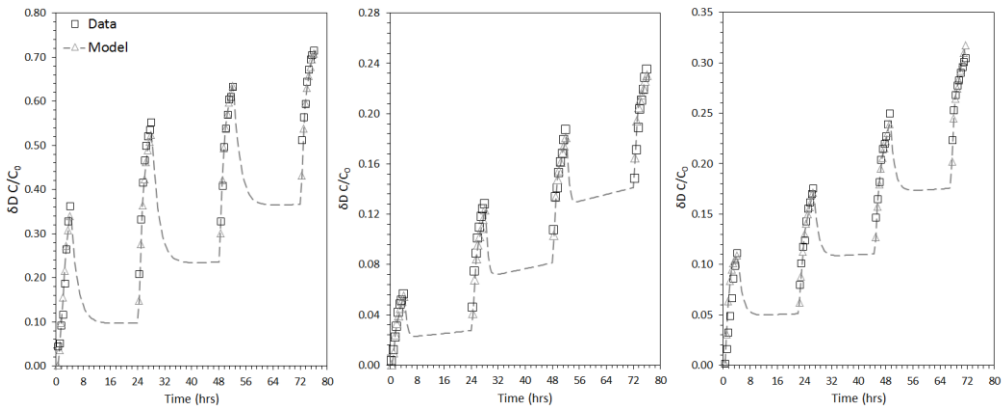


Figure 1. Normalised D<sub>2</sub>O breakthrough data along with best fit dual porosity model output for the interrupted-flow experiments conducted using core samples taken from 5.03 m (left), 9.52 m (middle) and 21.75 m (right) depth BGL.

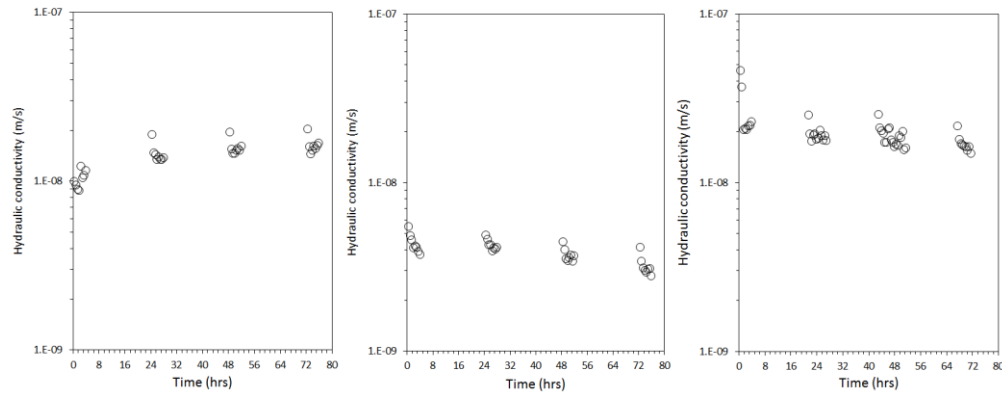


Figure 2. Vertical hydraulic conductivity (m/s), calculated using Eq. 2, for the interrupted-flow experiments conducted using core samples taken from 5.03 m (left), 9.52 m (middle) and 21.75 m (right) depth BGL.

Core depth (m BGL)	Core diameter, $D$ (mm)	Core length, $L$ (mm)	Total porosity, $\phi$	Pore volume of the mobile domain per total core volume, $\phi_m$	Coefficient of molecular diffusion, $\mu$ [ $L^2T^{-1}$ ]	Hydrodynamic dispersivity, $\alpha$ [L]	Mass transfer coefficient, $\gamma$ [ $T^{-1}$ ]	Half width of the matrix block, $a$ (mm)
--------------------	-------------------------	-----------------------	------------------------	--	---	---	--	--

Formatted: French (France)

Formatted: French (France)

5.03	100	36	0.44	0.06	$3.43 \times 10^{-5}$	$L_c/2$	0.65	18.3
9.52	100	47	0.47	0.04	$3.43 \times 10^{-5}$	$L_c/2$	1.50	12.1
21.75	100	55	0.43	0.08	$3.43 \times 10^{-5}$	$L_c/2$	1.20	12.3

Table 2. Constrained ( $D$ ,  $L_c$ ,  $\phi$ ,  $\mu$ ) and unconstrained ( $\phi_m$ ,  $\alpha$  and  $\gamma$ ) model parameters.  $a$  is calculated using Eq. 10.

Model output for the mobile and immobile domains at the top, middle and base of the core samples is displayed in Fig. 3. It is noted that for all core samples diffusion into the immobile domain during the induced flow periods is relatively significant, with  $\delta D_{im}/\delta D_m$  at the end of the first centrifugation (induced flow) period recorded as 0.16, 0.32 and 0.34 for the base of the core samples taken from 5.03 m, 9.52 m and 21.75 m depth BGL respectively. With respective average flow rates recorded as 0.017 m/d, 0.007 m/d and 0.015 m/d this behaviour is not obviously related to the variation in flow rates between the samples, but more likely to the intrinsic properties of the preferential flow domain (namely:  $\phi_m$ ,  $\gamma$  and  $\alpha$ ). It is also noted that for all core samples full equilibration between the mobile and immobile domains occurred ( $\delta D_{im} = \delta D_m$ ) during each no flow period. For example,  $\delta D_{im}$  and  $\delta D_m$  were modelled to be within  $\pm 1\%$  of each other after 7.0, 2.6 and 6.1 hrs during the first no flow period for the core samples taken from 5.03 m, 9.52 m and 21.75 m depth BGL respectively.

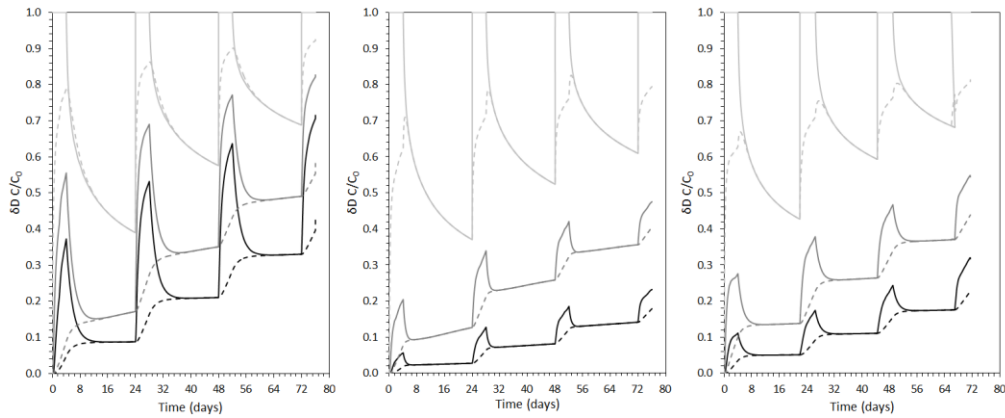


Figure 3. Model output for mobile (solid lines) and immobile (dashed lines) domains for core samples taken from 5.03 m (left), 9.52 m (middle) and 21.75 m (right) depth BGL. The black,

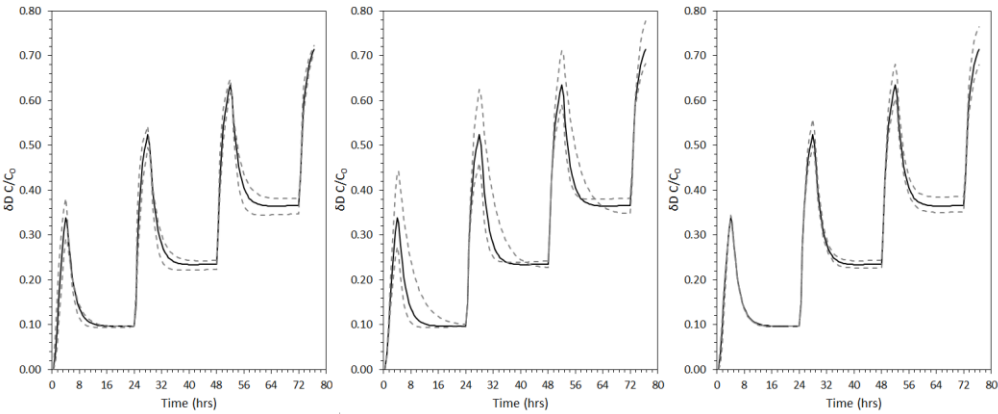
366 dark grey and light grey lines comprise model output for the base, middle and top of the cores  
367 respectively.

368 **3.53. Sensitivity analysis**

369 Sensitivity analysis plots for a  $\pm 50\%$  change in unconstrained parameters ( $\alpha$ ,  $\gamma$  and  $\phi_m$ ) for  
370 the core sample taken from 5.03 m depth BGL are displayed in Fig. 4, with corresponding  
371 NSMEC data displayed in Table 3. The model fitting efficiency is relatively insensitive to all  
372 three unconstrained parameters in the range tested, with a less than 12% change in the  
373 NSMEC compared to the NSMEC recorded for the best fit (Table 3). Sensitivity for the  
374 estimated % error associated with constrained parameters ( $\phi$ ,  $L$  and  $\mu$ ) are displayed in Fig. 5,  
375 with corresponding NSMEC data displayed in Table 3. The model fitting efficiency is also  
376 relatively insensitive, with a less than 1% change in the NSMEC compared to the NSMEC  
377 recorded for the best fit (Table 3). For the data presented the relatively low sensitivity to the  
378 parameters indicates that further testing, such as by dye tracing or geophysical tomography, is  
379 necessary to resolve more precisely the nature of the preferential flowpaths. Nevertheless, the  
380 modelling has supported the preferential flow conceptual model we have used to explain the  
381 step changes in concentration observed after resting periods. It has also provided a first order  
382 approximation of the likely geometry of the flowpaths.

383

384



385 Figure 4. Sensitivity of the dual domain model for the core sample taken from 5.03 m depth  
386 BGL due to  $\pm 50\%$  change in unconstrained parameters:  $\phi_m$  (LHS),  $\gamma$  (middle) and  $\alpha$  (RHS).

Model	Pore volume	Mass transfer	Hydrodyn	Total	Core	Coefficien
-------	-------------	---------------	----------	-------	------	------------

Parameter	of the mobile domain per total pore volume, $\phi_m$	coefficient, $\gamma$	amic dispersivity, $\alpha$	porosity, $\phi$	length, $L$	t of molecular diffusion, $\mu$
NSMEC (+ change)	0.925	0.926	0.952	0.974	0.965	0.964
NSMEC (- change)	0.952	0.862	0.964	0.968	0.971	0.975

Table 3. NSMEC for the core sample taken from 5.03 m depth BGL due to changes in constrained ( $L$ ,  $\phi$ ,  $\mu$ ) and unconstrained ( $\phi_m$ ,  $\alpha$  and  $\gamma$ ) model parameters. Changes in constrained parameters comprised the estimated percentage error per each parameter, which was 2.78%, 2.79% and 50% for  $L$ ,  $\phi$  and  $\mu$  respectively. Changes in unconstrained parameters were  $\pm 50\%$ . The NSMEC for the best fit was 0.972.

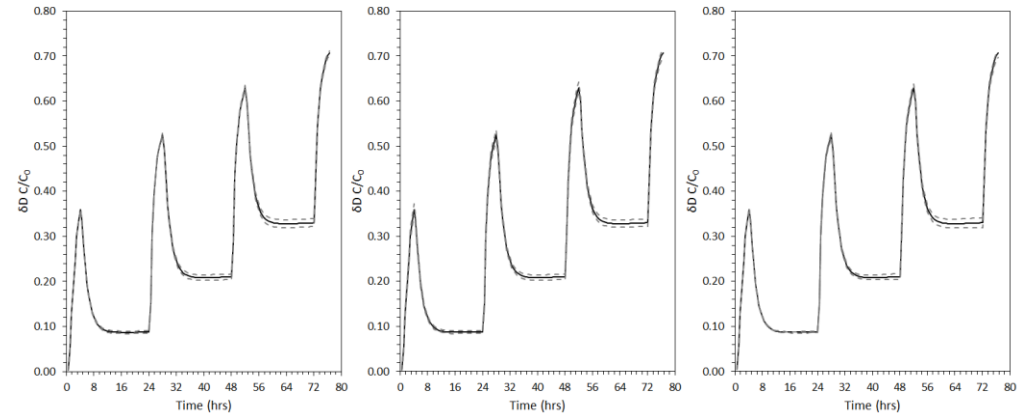


Figure 5. Sensitivity of the dual domain model for the core sample taken from 5.03 m depth BGL for the calculated error associated with the constrained parameters:  $\phi$  (LHS);  $L$  (middle) and  $\mu$  (RHS).

### 3.4 Comparison of dual and single domain modelling

In order to further demonstrate the practicality of the interrupted flow methodology, a numerical experiment was carried out using the dual domain model developed above. Using the best fit parameters from the core from 9.52 m depth BGL, an equivalent simulation to

Formatted: Font: Bold

the laboratory experiment described above was run, but *without* interrupted flow phases. The breakthrough curve produced was then fit to the Ogata-Banks equation (Ogata and Banks, 1961) on the assumption that flow was occurring only through a single domain. The resulting fitted was good (3% RMSE) with just one fitting parameter being the dispersion term -which yielded a ~~seemingly~~ reasonable value of  $(1.27 \times 10^{-8} \text{ m}^2/\text{s})$ . This illustrates that, without the use of interrupted flow phases to reveal the disequilibrium between two or more flow domains, a false assumption could easily be made with regard to the structure and associated transport properties of the core on the basis of a simple 1-D analytical model. This- could have very significant consequences for the prediction and management of solute migration through such deposits.

#### 4. Conclusions and outlook

Solute transport in the subsurface can be influenced by multiple nonlinear, rate-limited processes, and it is often difficult to determine which processes predominate for any given system. In this work we demonstrate the utility of interrupted-flow solute transport experiments using a CP to quantify the relative contributions of preferential flow pathways and surrounding matrix porosity to mass transfer processes in low permeability dual porosity materials. Dual domain transport modelling was used to validate the hypothesis that the step changes in tracer concentrations observed during no-flow periods could be explained by the presence of dual porosity in the samples. The modelling also enabled a first order approximation of the aspects of the physical properties of the two domains to be inferred. Smectite clay core samples were used (101.6 mm in diameter) as an example low  $K$  dual porosity media, however, it is anticipated that the methodology would also be suitable for the characterisation of any dual porosity material where mass transfer occurs via both advection and diffusion (e.g. fractured rock, heterogeneous soils, mine tailings). The methodology entails a minimum of three phases: induced flow, no flow, and induced flow, however, this may be repeated several times in order to most effectively characterise the multi-rate mass transfer behaviour. In addition, it is necessary to tailor the induced flow rate, interrupted-flow timescales and non-reactive tracer concentrations in order to most effectively identify different mass transfer processes whilst also simulating realistic total stress conditions. Future work will seek to further investigate the structure of the clay samples studied using quantitative tomography techniques (e.g. X-ray computed tomography and magnetic resonance imaging) and how these physical features can be integrated into site scale numerical flow modelling.

## Acknowledgements

The authors would like to thank Dayna McGeeney (School of Civil and Environmental Engineering) and Mark Whelan (School of Mining Engineering) from the Connected Waters Initiative Research Centre, UNSW, Australia, for their technical support. The work was financially supported by Program 1B of the National Centre for Groundwater Research and Training, supported by the Australian Research Council and the National Water Commission, and the Gary Johnson Trust. Dr Mark Cuthbert was financially supported by the European Community's Seventh Framework Programme [FP7/2007–2013] under grant agreement No.299091.

## References

- ASTM. Standard practice for thin-walled tube sampling of soils for geotechnical purposes. ASTM D1587-08(2012)e1, West Conshohocken, PA, 2012.
- ASTM. Standard test method for determining unsaturated and saturated hydraulic conductivity in porous media by steady-state centrifugation. ASTM D6527, West Conshohocken, PA, 2000.
- Barnes, C. J., Allison, G. B.: Tracing of water movement in the unsaturated zone using stable isotopes of hydrogen and oxygen. *Journal of Hydrology.*, 100, 143-176, 1988.
- Bashar, K., Tellam, J. H.: Non-reactive solute movement through saturated laboratory samples of undisturbed stratified sandstone. *The Geological Society of London Special Publications.*, 263, 233-251, 2006.
- Bear, J. Bachmat, Y. *Introduction to Modeling of Transport Phenomena in Porous Media.* Springer Science & Business Media. ISBN: 0792305574, 1990.
- Beven, K., Germann, P.: Macropores and water flow in soils. *Water Resources Research.*, 18, 1311-1325, 1982.
- Brusseau, M. L., Hu, Q., Srivastava, R.: Using flow interruption to identify factors causing nonideal contaminant transport. *Journal of Contaminant Hydrology.*, 24, 205–219, 1997.
- Brusseau, M. L., Rao, P. S. C., Jessup, R. E. and Davidson, J. M.: Flow interruption: a method for investigating sorption nonequilibrium. *J. Contam. Hydrol.*, 4, 223 240, 1989.

Formatted: English (U.S.)

466 Buczko, U, Hopp, L., Berger, W., Durner, W., Peiffer, S., Scheithauer, M.: Simulation of  
 467 chromium transport in the unsaturated zone for predicting contaminant entries into the  
 468 groundwater. *Journal of Plant Nutrition and Soil Science.*, 167, 284-292, 2004.

469 Coats, K. H., Smith, B. D.: Dead-end pore volume and dispersion in porous media. *Soc. Pet.*  
 470 *Eng. J.*, 4, 73–84, 1964.

471 Cote, C. M., Bristow, K. L., Ross, P. J.: Increasing the efficiency of solute leaching: impacts  
 472 of flow interruption with drainage of the “preferential flow paths.” *Journal of Contaminant*  
 473 *Hydrology.*, 43, 191-209, 2000.

474 Cote, C. M., Bristow, K. L., Ross, P. J.: Quantifying the Influence of Intra-Aggregate  
 475 Concentration Gradients on Solute Transport. *Soil Science Society of America Journal.*, 63,  
 476 757-767, 1999.

477 Cuthbert, M. O., Mackay, R., Tellam, J. H. Thatcher, K. E.: Combining unsaturated and  
 478 saturated hydraulic observations to understand and estimate groundwater recharge through  
 479 glacial till. *Journal of Hydrology.*, 391(3), 263-276, 2010.

480 Cuthbert, M.O, and C Tindimugaya.: The importance of preferential flow in controlling  
 481 groundwater recharge in tropical Africa and implications for modelling the impact of climate  
 482 change on groundwater resources. *Journal of Water and Climate Change.*, 1(4), 234-245,  
 483 2010.

484 Cuthbert, M.O., R Mackay, JR Nimmo.: Linking soil moisture balance and source-responsive  
 485 models to estimate diffuse and preferential components of groundwater recharge. *Hydrology*  
 486 *and Earth System Sciences.*, 17(3), 1003-1019, 2013.

487 Flury, M., Fluhler, H., Jury, W. A., Leuenberger, J.: Susceptibility of soils to preferential  
 488 flow of water: [Aa](#) field study. *Water Resources Research.*, 30, 1945-1954, 1994.

489 Gerke, H. H., van Genuchten, M. T.: Evaluation of a first-order water transfer term for  
 490 variably saturated dual-porosity flow models. *Water Resources Research.*, 29(4), 1225–1238,  
 491 1993.

492 Gong, R., Lu, C., Wu, W.-M. Cheng, H., Gu, B., Watson, D.B., Criddle, C.S., Kitanidis,  
 493 P.K., Brooks, S.C., Jardine, P.M. Luo, J.: Estimating kinetic mass transfer by resting-period  
 494 measurements in flow-interruption tracer tests. *Journal of Contaminant Hydrology.*, 117, 37-  
 495 45, 2010.

496  
 497 Guimont, S., Perrin-ganier, C., Real, B., Schiavon, M.: Effects of soil moisture and treatment  
 498 volume on bentazon mobility in soil. *Agronomy for Sustainable Development.*, 25, 323-329,  
 499 2005.

500 Hensley, P. J., and Schofield, A. N.: Accelerated physical modelling of hazardous-waste  
 501 transport. *Geotechnique.*, 41(3), 447–465, 1991.

502 Nash, J. E., Sutcliffe, J. V.: River flow forecasting through conceptual models part I — A  
 503 discussion of principles., *Journal of Hydrology*. 10(3), 282–290, 1970.

504 Koch, S., Fluhler, H.: Non-reactive solute transport with micropore diffusion in aggregated  
 505 porous media determined by a flow-interruption method. *Journal of Contaminant Hydrology*.,  
 506 14, 39-54, 1993.

507 Ma, L., Selim, H. M.: Solute transport in soils under conditions of variable flow velocities.  
 508 *Water Resources Research*., 32, 3277-3283, 1996.

509 Murali, V. and Aylmore, L. A. G.: No-flow equilibrium and adsorption dynamics during  
 510 ionic transport in soils. *Nature (London)*., 283, 467-452, 1980.

511 Nimmo, J. R., and K. A. Mello.: Centrifugal techniques for measuring saturated hydraulic  
 512 conductivity. *Water Resources Research*., 27(6), 1263–1269, 1991.

513 [Ogata, A., Banks, R. B.: A solution of the differential equation of longitudinal dispersion in](http://pubs.usgs.gov/pp/0411a/report.pdf)  
 514 [porous media. \*Fluid Movement in Earth Materials\*, Geological Survey Professional Paper.,](http://pubs.usgs.gov/pp/0411a/report.pdf)  
 515 [411-A. <http://pubs.usgs.gov/pp/0411a/report.pdf>](http://pubs.usgs.gov/pp/0411a/report.pdf)

516 Orr, W. J. C., Butler, J. A. V.: The rate of diffusion of deuterium hydroxide in water. *J.*  
 517 *Chem. Soc.*, 303, 1273-1277, 1935.

518 Reedy, O. C., Jardine, P. M., Wilson, G. V. and Selim, H. M.: Quantifying the diffusive mass  
 519 transfer of nonreactive solutes in columns of fractured saprolite using flow interruption. *Soil*  
 520 *Sci. Soc. Am.*, 60(5), 1376–1384, 1996.

521 Shukla, M. K., Lal, R., Owens, L. B. and Unkefer, P.: Land use and management impacts on  
 522 structure and infiltration characteristics of soils in the North Appalachian region of Ohio. *Soil*  
 523 *Science*., 168(3), 167-177, 2003.

524 Sundaram, B., Feitz, A., Caritat, P. de, Plazinska, A., Brodie, R., Coram, J. and Ransley, T.:  
 525 *Groundwater Sampling and Analysis – A Field Guide*. Geoscience Australia, Record 2009/27  
 526 95, 2009.

527 Timms, W. A., Crane, R. A., Anderson, D. J., Bouzalakos, S., Whelan, M., McGeeney, D.,  
 528 Rahman, P. F., Guinea, A., and Acworth, R. I.: Vertical hydraulic conductivity of a clayey-  
 529 silt aquitard: accelerated fluid flow in a centrifuge permeameter compared with in situ  
 530 conditions. *Hydrology and Earth System Sciences Discussion*. 11, 3155-3212, 2014.

531 Timms, W., Hendry, M.: Long-term reactive solute transport in an aquitard using a centrifuge  
 532 model. *Ground Water*., 46, 616-628, 2008.

533 Timms, W., Hendry, M.J., Muise, J., Kerrich, R.: Coupling centrifuge modeling and laser  
 534 ablation inductively coupled plasma mass spectrometry to determine contaminant retardation  
 535 in clays. *Environ. Sci. Technol.*, 43, 1153–1159, 2009.

**Formatted:** Font: Times New Roman,  
12 pt

536 Totsche, K. U., Jann, S., Kogel-Knabner, I.: Release of polycyclic aromatic hydrocarbons,  
537 dissolved organic carbon, and suspended matter from disturbed NAPL-contaminated gravelly  
538 soil material. *Vadose Zone Journal.*, 5, 469-479, 2006.

539 Wehrer, M., Totsche, K. U.: Detection of non-equilibrium contaminant release in soil  
540 columns: Delineation of experimental conditions by numerical simulations. *Journal of Plant*  
541 *Nutrition and Soil Science.* 116, 475-483, 2003.

542 Wehrer, M., Totsche, K. U.: Determination of effective release rates of polycyclic aromatic  
543 hydrocarbons and dissolved organic carbon by column outflow experiments. *European*  
544 *Journal of Soil Science.*, 56, 803-813, 2005.

545 Wehrer, M., Totsche, K. U.: Difference in PAH release processes from tar-oil contaminated  
546 soil materials with similar contamination history. *Chemie de Erde – Geochemistry.*, 69, 109-  
547 124, 2009.

548 Wilson, J. L., and L. W. Gelhar.: Analysis of longitudinal dispersion in unsaturated flow 1.  
549 The analytical method, *Water Resour. Res.*, 17(1), 122– 130, 1981.

550

551

552

553

554

555

556

557

558

559

560

561

562

563

564

565

Second response to referee comments for “Technical Note: The use of an interrupted-flow centrifugation method to characterise preferential flow in low permeability media” by R. A. Crane et al.

**Our second responses are included in bold and blue text.**

Many thanks to Anonymous Referee #1 for giving their time to provide comments on our manuscript. Please see below for our responses to your questions/comments.

#### **Anonymous Referee #1**

I am not sure of the usefulness of the method. Curve fitting numerical solutions of 2 PDE's with 3 available parameters is far from trivial and nothing is given to really help the user in doing it. My suggestion is that since the method would be used in practice only if curve fitting is easy and since they fit only the rising limb of the breakthrough curve it should not be too difficult to provide a good analytical approximation. Not only this would make the method useful it would also show the reader the physical influence of the parameters. As is I really learned very little physically.

Thank you for this comment on the modelling aspect of the paper. However, the central “thrust” of this research is in presenting the empirical methodology (i.e. the interrupted flow centrifugation technique), with the shape of the non-reactive tracer breakthrough curve alone being an indicator of dual porosity flow occurring in the geological media. The numerical modeling was therefore used as a complimentary technique to confirm whether the shape of curve was indicative of dual porosity behavior. As such, the whole breakthrough curve was fitted, not just the rising limb as the reviewer suggests but also the decrease in concentration during the resting phases, and an analytical solution is unfortunately not tractable for this case. Future work will seek to develop both the empirical and numerical elements of the research in order to improve the applicability of the technique and its physical inference.

**Nevertheless, to try and address the reviewer's concern we have carried out some additional modelling and analysis to strengthen the case for the importance of the interrupted flow observations and added a new section to the manuscript as follows (Line 387 to 399):**

#### **“3.4 Comparison of dual and single domain modelling**

**In order to further demonstrate the practicality of the interrupted flow methodology, a numerical experiment was carried out using the dual domain model developed above. Using the best fit parameters from the core from 9.52 m depth BGL, an equivalent simulation to the laboratory experiment described above was run, but *without* interrupted flow phases. The breakthrough curve produced was then fit to the Ogata-Banks equation (Ogata and Banks, 1961) on the assumption that flow was occurring only through a single domain. The**

resulting fitted was good (3% RMSE) with just one fitting parameter being the dispersion term which yielded a reasonable value of  $1.27 \times 10^{-8} \text{ m}^2/\text{s}$ . This illustrates that, without the use of interrupted flow phases to reveal the disequilibrium between two or more flow domains, a false assumption could easily be made with regard to the structure and associated transport properties of the core on the basis of a simple 1-D analytical model. This could have very significant consequences for the prediction and management of solute migration through such deposits.”

Second response to referee comments for “Technical Note: The use of an interrupted-flow centrifugation method to characterise preferential flow in low permeability media” by R. A. Crane et al.

**Our second responses are included in bold and blue text.**

Many thanks to Anonymous Referee #2 for giving their time to provide comments on our manuscript. Please see below for our responses to your questions/comments.

## **Anonymous Referee #2**

### **1 General comments**

The manuscript proposes a novel method to characterise preferential flow in low permeability media with preferential flow paths. The method is given by a combination of an experimental and a modelling phase. The experimental phase consists in performing laboratory transport tests using the interrupted-flow centrifugation method. The modelling phase consists in fitting the experimental results with a dual domain model which is a variant of the dual porosity model considering also the molecular diffusion in the immobile domain. The method is applied to three samples of smectite clay dominated samples, with diameter around 10 cm and height between 3 and 5 cm. The results show that the dual domain model fits very well the experimental data and that the model fitting efficiency is relatively insensitive to the model parameters. The conclusion is that the method proposed is a powerful method to characterise preferential flow in low permeability media. I think that the subject is of interest to the scientific community: as stated by the authors, the hydraulic properties of aquitards are important, as the presence of preferential flow paths can compromise their integrity as barriers to the movement of groundwater contaminants. The method proposed in this paper has the objective of characterizing the dual porosity behaviour of such porous media. The article is well structured, well written, concise and generally clear. The objectives are clearly stated both in the abstract and in the introduction, where a good list of references is given to introduce the subject. Therefore, I recommend this manuscript for publication, after some minor revisions suggested in the following.

**Minor changes have been made to improve the written quality of the introduction, namely lines 89-95 in the original manuscript, see tracked changes.**

I have some doubts about the applicability of the method to practical situations. Specifically:

- I wonder at which scale this method can be applied. The samples diameter is around 10 cm and their height between 3 and 5 cm. Can the best fit parameters obtained at this scale be used to model transport at larger scale?

This is a good question, but beyond the scope of this paper – it can only be effectively answered, with the integration of the results from this work with well constrained field data, which is something we are now working on for a future paper. However, as we note in the current paper, a key benefit of the use of a relatively large centrifuge permeameter (100 mm diameter) for this method is their ability to house large samples compared to conventional core testing (~20 to 30 mm

diameter). This has provided a unique capability to identify dual porosity at a scale of centimeters that would be difficult or impossible to quantify at other scales.

- Does the centrifugation affect the structure of the porous medium, i.e., the connectivity of the preferential flow paths?

Whether or not there is significant alteration of porous structure depends upon a wide range of complex physical and chemical factors associated with the core and the centrifuge induced stress environment. In this work, in order to minimize any unnatural physical effects such as new or enhanced preferential flow paths, the maximum centrifuge g-level was set at slightly less than the estimated in situ stress of the core sample at the depth from which it was extracted. Maximum stress to prevent deformation of the core was estimated assuming that the overlaying formations were fully saturated and of the same density to the core samples, using Equations 3 and 4 (see Section 2.2.). In addition, this centrifuge permeameter was designed to position at a relatively large centrifuge radius of 0.65 m to reduce stress differences (due to g-level) between the base and top of the core, compared with small centrifuge permeameters.

- One of the conclusions of the paper is that the modelling enabled aspects of the physical properties of the two domains to be inferred. Moreover, the model fitting is shown to be relatively insensitive to the model parameters; can this fact weaken the former conclusion?

The numerical modeling was used as a complimentary technique to confirm whether the shape of curve was indicative of dual porosity behavior. The parameter with the greatest sensitivity was the mass transfer coefficient which is also the parameter which lends greatest insight into the likely geometry of the preferential flow paths. So, in that sense, we consider the conclusion that aspects of the physical properties of the two domains can be inferred from the model is sound. However, we have noted in the text that further work is needed to clarify the relationship between the model parameters and the physical structure of the cores by other methods.

**We have added a new paragraph at Lines 367 to 372 (of the original manuscript file) as follows:**

**“For the data presented the relatively low sensitivity to the parameters indicates that further testing, such as by dye tracing or geophysical tomography of some kind, is necessary to resolve more precisely the nature of the preferential flowpaths. Nevertheless, the modelling has supported the preferential flow conceptual model we have used to explain the step changes in concentration observed after resting periods. It has also provided a first order approximation of the likely geometry of the flowpaths.”**

**We have also amended the text (in italics below) in Lines 408 to 409 (of the original manuscript file) to make this source of uncertainty clearer as follows:**

**“The modelling also enabled a *first order approximation* of the physical properties of the two domains to be inferred”**

737

738 Page 70, line 23: I suggest to modify the sentence in 'the possible dual porosity  
739 behaviour' or in 'low permeability porous media characterised by the presence of  
740 preferential flow path'. In fact, if the low permeability porous medium is  
741 homogeneous, then it does not show any dual porosity behaviour.

742

743 Yes, we agree and have now added the word 'possible' before dual porosity as the  
744 reviewer suggests.

745

746 • Page 72, line 3: I think it should be specified somewhere in this section that three  
747 core samples were analysed, each one coming from a different depth.

748

749 We agree and have added an additional sentence in Page 23 Line 4:

750

751 In total three core samples were analysed, which were taken from depths of 5.03,  
752 9.52 and 21.75 m BGL.

753

754 • Page 72, lines 16-19: Is there a reason why the clay cores are taken larger  
755 than the core holder and then trimmed, instead of taking directly a clay core of  
756 the needed diameter? I think some more explanations would be useful here.  
757 Moreover, I think the sentence should be rephrased, as it seems that the subject  
758 of the verb 'inserted' is 'the outer 5 mm of the clay cores'.

759

760 We agree and have now added the following sentence to Line 19:

761

762 "The cores were trimmed in order to remove any physical and chemical disturbance  
763 associated with the core extraction (drilling) process and to ensure a close fit with the  
764 permeameter liner."

765

766 We have also changed Lines 16-19 to:

767

768 "Prior to mounting into the CP the outer 1.6 mm of the clay cores were trimmed and  
769 the trimmed cores were then inserted into Teflon cylindrical core holders (100 mm  
770 internal diameter, 220 mm length) using a custom built mechanical cutting and  
771 loading device."

772

773 This makes it clear that the trimmed cores were inserted into the core holders rather  
774 than the trimmed material.

775

776 • Page 74, line 20 (and following): I think it should be clearly distinguished between  
777 the different dual domain approaches in order to correctly situate the  
778 model introduced by the author in the existing literature. In particular, Coats  
779 and Smith (1964) and van Genuchten and Wierenga (1976) introduce a model  
780 of mobile/immobile type (which I would call dual porosity model). On the other  
781 hand, the model introduced by Gerke and van Genuchten (1993, 1993a) is not a  
782 mobile/immobile model, as water can flow in both domains (with different velocities)  
783 and so the solute can be transported by advection and by dispersion in both  
784 domains. This kind of models is more correctly called 'dual permeability model' (see,  
785 e.g., Baratelli et al 2014 for more references to the two different modeling

approaches). The model introduced by the authors is closer to the dual-porosity mobile/immobile approach.

We agree that it is important to be clear that the model presented is a “dual porosity” model and not a “dual permeability” model. We have therefore removed the reference to Gerke & van Genuchten (1993) at this point in the manuscript which is presumably the source of the reviewer’s concern since, as they correctly point out, it refers to a dual permeability approach.

• Page 76, equations (5)-(7): I think the authors should clearly state how their model is ‘novel’ (Page 70, line 23) with respect to the model already existing in the literature. I guess the novelty is mainly related to the presence of the molecular diffusion term in the immobile domain; it would be interesting to add some explications to justify this choice.

We stated in the text (p.76, lines 3-7) that the main novelty in the model formulation which is the setup of the upper boundary condition switching during the flow and rest phases respectively. Hence, we’re not sure what the reviewer’s concern is here. However we have clarified the boundary conditions as described in our reply to the next comment by the reviewer “Page 76, lines 1-9: I think that the boundary conditions used are not very clear.”

• Page 76, lines 1-9: I think that the boundary conditions used are not very clear. In particular, the flow is not simulated and so the boundary conditions for flow (line 1) are not required. Moreover, it would be useful to explain more clearly the boundary conditions applied at the top and bottom of the column for both the mobile and immobile domain.

Yes, we agree this section needs clarification and the mention of a flow boundary condition was misleading (we had explicitly included the flow equations in an earlier iteration, but not for the results finally presented here). We have now clarified this section (originally p76, lines 1-9) to read:

“The initial concentration conditions were set to zero for both domains for all model runs. During centrifugation periods, a variable solute flux upper boundary condition was used for the mobile domain varied according to the product of the measured fluid flux & input concentration ( $C_0$ ) during each experiment as follows:

$$\frac{q(t)}{\phi_m} C_0 = \frac{q(t)}{\phi_m} C_m + D_m \frac{\partial C_m}{\partial z}$$

A Dirichlet (constant concentration) upper boundary condition was used for the immobile domain during times of centrifugation. A novel aspect of the models, facilitated by the flexibility of model structure variations possible in COMSOL, was that the upstream transport boundary for both domains was switched to a zero flux condition during the interrupted flow phases. The downstream transport boundary conditions for both domains were given by:

$$\frac{\partial C_{m,im}}{\partial z} = 0$$

At  $z = L$ , where  $L$  was sufficiently large to ensure the results at the column outlet distance (at  $z \ll L$ ) were not sensitive to the position of the boundary.”

• Page 78, line 22-23: It would be interesting to explain the implications of this result.

We have attempted to do this in the text on p.78 lines 24-28.

• Page 79, line 3-4: Is the choice of using the same  $\alpha$  as for parallel fracture geometry justified?

Good question! In order to show the range of uncertainty associated with this geometry factor we have now included a range of inferred values of  $\alpha$  using Beta values for parallel slabs (Beta = 3) as well spherical aggregates (Beta =15).

### 3 Technical corrections

• Page 72, line 7: Correct ASTM 2012 with ASTM (2012).

We have now corrected this.

• Page 72, lines 11-12: I suggest to explicitly define the symbols EC and Eh, although I understand that it is a rather standard notation.

We have now defined these symbols, see tracked changes.

• Page 72, equation (2): It seems to me that the results has the unit of  $[1/T]$  and not of  $[L/T]$  as I would expect for the hydraulic conductivity.

Equation 2 gives dimensions of K of  $[L/T]$ , following the detailed derivation provided in ASTM 2000 and Timms et al. (2014). Equation 2 is expressed for laboratory convenience in terms of RPM rather than more standard parameters, Dimensions for  $(RPM)^2$  of  $[1/L]$  is obtained, such as equation 5 of Timms et al. (2014), by rearranging  $a/g = 0.001.r.(RPM)^2$ . The  $[1/L]$  dimensions of  $RPM^2$  then cancel with the other dimensions in Equation 2 of this paper to give K with dimensions of  $[L/T]$  as expected.

• Page 72, equation (2): I think K should be substituted by Kv, as in the following the hydraulic conductivity is always indicated as Kv without being explicitly defined (see page 78, Table 1, ...).

We have now changed this.

• Page 76, line 2: exchange -> exchanged.

We have now changed this.

• Page 76, line 28: I think that  $\alpha$  should be corrected with  $\alpha_T$ .

879 The notation we have used for the total porosity here is consistent with how we  
880 defined it on p75 line 10, so we don't think it needs changing.

881  
882 • Page 78, line 19: I suggest to add a comma between '0.43' and 'this'.

883  
884 We have now changed this.

885  
886 • Page 82, line 21: afield -> a field.

887 We have now changed this.

888

889